Published at http://dx.doi.org/10.1109/JLT.2017.2674308

Throughput Gains from Adaptive Transceivers in Nonlinear Elastic Optical Networks

David J. Ives, *Member, OSA*, Alex Alvarado, *Senior Member, IEEE*, and Seb J. Savory, *Fellow, IEEE, Fellow, OSA*

(Invited Paper)

***Abstract*—In this paper we link the throughput gains, due to transceiver adaptation, in a point-to-point transmission link to the expected gains in a mesh network. We calculate the maximum network throughput for a given topology as we vary the length scale. We show that the expected gain in network throughput due to transceiver adaptation is equivalent to the gain in a point-to-point link with a length equal to the mean length of the optical paths across the minimum network cut. We also consider upper and lower bounds on the variation of the gain in network throughput due to transceiver adaptation where integer constrained channel bandwidth assignment and quantized adaptations are considered. This bounds the variability of results that can be expected and indicates why some networks can give apparently optimistic or pessimistic results. We confirm the results of previous authors that show finer quantization steps in the adaptive control lead to an increase in throughput since the mean loss of throughput per transceiver is reduced. Finally we consider the likely network advantage of digital nonlinear mitigation and show that a significant trade off occurs between the increase in SNR for larger mitigation bandwidths and the loss of throughput when routing fewer large bandwidth superchannels.**

***Index Terms*—Optical fiber communication, optical fiber networks, adaptive modulation, flexible networks.**

I. Introduction

TRANSPARENT wavelength routed optical networks form the backbone of data transport across the Internet. With increasing demand for data services such networks must be optimized to maximize the utilization of resources, to transport more data on the existing optical fiber infrastructure.

In this paper we consider a transparent wavelength routed optical network with routing in the optical domain carried out by virtue of the signal wavelength. We will assume that there is no optical regeneration or wavelength conversion between the transmitter and receiver. We are considering a network where fiber resources are at a premium such that data is transmitted using the latest coherent optical technology with spectrally efficient modulation formats and coding schemes and are able to equalize linear distortions electronically.

Manuscript received month dd, 20YY; revised month dd, 20YY. This work was supported by the UK Engineering and Physical Sciences Research Council through programme grant UNLOC [EP/J017582/1] and project INSIGHT [EP/L026155/1].

D. Ives and S. Savory are with the University of Cambridge, Department of Engineering, 9 JJ Thomson Ave, Cambridge CB3 0FA, UK. (e-mail: di231@cam.ac.uk; sjs1001@cam.ac.uk).

A. Alvarado is with the Signal Processing Systems (SPS) Group, Department of Electrical Engineering, Eindhoven University of Technology, 5600 MB Eindhoven, The Netherlands. (e-mail: alex.alvarado@ieee.org)

Physical layer transmission impairments, caused by stochastic noise and nonlinear propagation, limit the quality and data capacity of the transmitted signals. The optical losses during transmission are compensated at regular intervals by basic amplification to maintain the signal power. This amplification adds stochastic noise to the signal while the weak nonlinear refractive index of optical fiber causes intra- and inter-channel interference. We consider dispersion uncompensated links and use the Gaussian Noise (GN) model of nonlinear interference [1]. The nonlinear interference grows with the launch power cubed and thus limits the maximum launch power and thus the maximum SNR and data capacity of the transmitted signal.

Software controlled network elements allow remote optimization of the use of network resources. Adaptive transceivers can alter the transmitted signal format to match the available transmission SNR and the required client data rates. Reconfigurable optical add drop multiplexers (ROADMs) using wavelength selective switches can be used to route the optical signals to maximize the utilization of the fiber resources.

To maximize the data transmitted over a given light path the transceivers can use basic modulation format adaptation [2], 4D modulation schemes [3], time division hybrid formats [4], OFDM subcarrier modulation adaptation [5], probabilistic shaping [6], [7] and FEC overhead (OH) adaptation [8]–[11]. The adaptation of the optical launch power [12], [13] and mitigation of nonlinear interference using, for example digital back propagation (DBP) [14], [15], can improve the properties of the light path. The use of flexible grids with adaptive signal bandwidth [16], superchannels and sliceable transceivers [17] allows the light path bandwidth to be better matched to the clients data requirements. With all of these the size of the adaptation control steps are important and it has been shown that finer steps improves network throughput [18], [19].

The potential of these techniques is easily simulated and demonstrated with point-to-point transmission. The question we would like to answer is how useful are such adaptation techniques in a network context? Also given limited resources for digital signal processing within the coherent transceivers which adaptation techniques are more effective?

The significant difference between a network and a point-to-point link is that there are multiple signal sources and destinations with in general multiple paths between them. As such a transceiver cannot have complete information about all the interfering signals that co-propagate with the transmission signal over part of the light path. The total data transported by a network also depends on the routing and wavelength

Published at http://dx.doi.org/10.1109/JLT.2017.2674308

constraints where to fairly divide the bandwidth may require unfeasible fractional channels. The signals also travel a variety of distances and accumulate different levels of impairments such that the transceiver adaptation has different advantages for signals transmitted over different light paths.

Understanding the advantages of adaptation in a network context has previously been estimated considering the adaptation as a perturbation to a previously calculated optimal routing and wavelength assignment (RWA) [20]. While in [21] the advantage of low loss, low nonlinearity fiber is estimated by considering each light path in isolation. These approaches can be inaccurate in a network where the advantage due to adaptation or physical layer performance depends on the light path length and thus to give all light paths a similar gain in throughput will require a redistribution of bandwidth and a change to the RWA solution. For larger networks heuristic Monte-Carlo based estimation techniques using sequential or dynamic demands have been used. Such techniques have been used to compare RWA algorithms [22], [23] and the advantages of adaptive networking [24], [25] for dynamic networks. Monte-Carlo techniques with sequential loading techniques have also been used [26] and more recently the SNAP, statistical network assessment process, algorithm [27] has been developed. The stochastic nature of the demands means the traffic matrix is less well defined and the RWA solution may skew towards more easily accommodated demands. This limitation could be overcome with a careful implementation of the Monte-Carlo approach.

In this work, that extends our previous paper [28], we assess the effect of adaptation on the network for an optimal RWA giving the maximum network throughput. The RWA is fully re-optimised for the unadapted and adapted case to compare optimal throughputs in both cases. The main contribution of this work is the comparison of the advantages of adaptation for a network with those of the more easily calculated point-to-point link. We illustrate the deviation from this point-to-point expectation of network throughput and investigate the lower and upper bounds on the throughput gains due to adaptation.

Section II outlines the physical layer impairment model used in this work, the definition of network data throughput along with the methods used to find the upper bounds and optimum throughput. Section III shows the throughput results of a number of simple adaptations in a point-to-point link and two network topologies. Finally in section IV we discuss global conclusions that can be drawn for the advantages of adaptive transceivers in nonlinear networks.

II. Background

A. Transmission Impairment Model

For the physical network we consider a transparent optical infrastructure composed of nodes formed of ideal (ROADMs) and links formed of a number of equal length fiber spans with erbium doped fiber amplifiers (EDFA) to compensate for the span loss. We consider polarization multiplexed coherent optical signals operating on a fixed 50 GHz grid, a total of 80 channels each of 32 GBaud Nyquist sinc pulses. It is assumed that linear impairments are ideally compensated at the receiver and that the only significant physical layer impairments are amplified spontaneous emission (ASE) noise from the EDFAs and nonlinear interference. The imperfections of non-ideal network components, for example crosstalk and optical filtering [29], [30], in the ROADMs along with PDL and EDFA imperfections, have not been included in this study.

TABLE I
FIBER PARAMETERS USED.

Parameter	Symbol	Value	
Span Length	L	80	km
Attenuation Coefficient	α	0.22	dB·km^{-1}
Chromatic Dispersion Coefficient	β_2	16.7	ps·nm^{-1}·km^{-1}
Nonlinear Coefficient	γ	1.3	W^{-1}·km^{-1}

The ASE noise accumulates linearly with the number of spans, where the additional noise per span in the receiver matched filter bandwidth, n_{ASE}, is given by

$$n_{ASE} = 10^{\frac{NF}{10}}\ h\nu\ 10^{\frac{\alpha L}{10}}\ R \tag{1}$$

where NF is the amplifier noise figure assumed to be 5 dB here, h is Plank's constant, ν is the optical carrier frequency of 193.5 THz, α is the optical fiber attenuation coefficient, L is the span length and R is the noise bandwidth of the receiver matched filter and for the assumed white noise is equal to the symbol rate. The fiber parameters used are shown in table I and lead to n_{ASE} = 0.7466 μW.

The nonlinear interference is estimated using the coherent GN model [1] assuming the links are fully loaded and all operating at the same launch power. For each light path the symbol SNR of the received signal, on the worst case central channel, is estimated as

$$SNR = \frac{p_0}{N_s\ n_{ASE} + N_s^{(1+\epsilon)}\ \eta\ p_0^3} \tag{2}$$

where p_0 is the launch power on all channels, N_s is the number of spans in the light path, η is the nonlinear interference coefficient and ϵ is the coherent addition factor. The nonlinear interference is the worst case impairing the central channel of a fully loaded DWDM transmission. Similar to the LOGON [31] approach the launch power p_0 was optimised to maximise the SNR on the central channel transmitted over a distance equal to the mean shortest path, for fully loaded DWDM transmission. The use of the fully loaded link assumption is expected to have a small detrimental effect on network performance. At the maximum network throughput the bottleneck links will be full and many other links are likely to be heavily loaded. In our previous study [32] of the NSF network topology, at maximum throughput, the effect of adapting individual launch powers only increased the received SNR by order 0.1 dB.

The nonlinear interference coefficient η was calculated for a transmitted power spectral density formed of 80 channels of 32 GBaud sinc pulses on a 50 GHz grid. Table I shows the fiber parameters assumed. The total nonlinear interference, $\eta\, p^3$, on the central channel was calculated by integrating the nonlinear interference power spectral density over the receiver match filter bandwidth [19, equation (3)]. The integration was carried out numerically using an importance sampled Monte-Carlo algorithm. The coherent accumulation factor ϵ was calculated

TABLE II
NONLINEAR INTERFERENCE COEFFICIENTS CALCULATED.

No. channels DBP	η [mW^{-2}]	ϵ	Symbol SNR at 2000 km [dB]
0	$9.149{\cdot}10^{-4}$	$6.207{\cdot}10^{-2}$	13.9
1	$7.444{\cdot}10^{-4}$	$1.927{\cdot}10^{-3}$	14.5
2	$6.632{\cdot}10^{-4}$	$1.426{\cdot}10^{-3}$	14.7
4	$5.917{\cdot}10^{-4}$	$1.370{\cdot}10^{-3}$	14.9

by comparing the numerical integration of the GN model for 100 spans with the η for a single span.

In the case where we consider digital nonlinear compensation of the intra-superchannel nonlinear interference we assumed that this is ideally removed from the total nonlinear interference. The nonlinear coefficient η represents the nonlinear interference on the worst channel within the worst superchannel. That is the outside channel within a superchannel that is in the centre of a fully loaded band. The outer most channel of a superchannel experiences the most nonlinear interference from the neighbouring superchannel while the central superchannel experiences the most nonlinear interference from the fully loaded band. Table II lists the nonlinear interference coefficients, coherence addition factor and SNR calculated after 2000 km of transmission for 0, 1, 2 and 4 channels of digital nonlinear mitigation.

B. Tested Topologies

In this work we consider three topologies to test the effects of transceiver adaptation. A simple point-to-point link, a 3-node linear network and a 9-node network based on the DT core topology [21]. For each topology the number of spans in each link will be varied to test the robustness of results and avoid any favorable or unfavorable result due a fortuitous length scale. Figure 1 illustrate the topologies considered and shows the link lengths relative to the reference link length. These networks are all small enough to solve optimally, either analytically or using integer linear programming (ILP) techniques in a reasonable time.

C. Ideal Transceiver Model

We consider an ideal AWGN Shannon capacity transceiver with the addition of a coding gap and quantized throughput rates. The transceiver throughput is given by

$$\theta = q \left\lfloor \frac{2}{q} \frac{R}{} \log_2\left(1 + \frac{SNR}{g}\right) \right\rfloor \tag{3}$$

where q is the quantization steps, in this work 100 Gb·s^{-1}, 25 Gb·s^{-1} and continuous with $q \to 0$. g is the coding gap to the ideal Shannon capacity, $g = 2$ represents a 3 dB coding gap and $g = 1$ for ideal Shannon capacity and R is the symbol rate. $\lfloor x \rfloor$ represents the largest integer less than x. The coding gap g represents how close the throughput of a practically transceiver is to the Shannon capacity while the quantization step q allows for the implementation of discrete rather than continuous adaptation of coding rates. The use of an ideal AWGN Shannon capacity transceiver allows investigation with both continuous and quantized rate adaptation. The ideal case with coding gap, $g = 1$, provides rates that are optimistic in comparison to practically achievable rates. The correct choice of g can better approximate practically achievable transmission rates. This variation in coding gap, g, rescales the received SNR and to first order rescales the distance axis in the results presented.

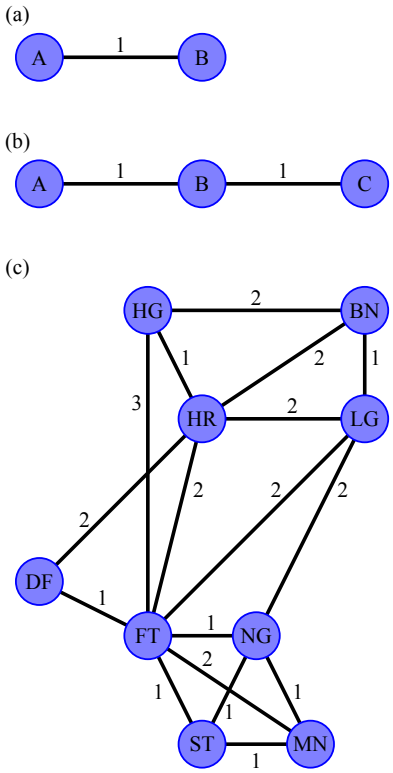

Fig. 1. Topologies considered. (a) a point-to-point link, (b) a 3-node linear network and (c) the 9-node mesh network considered, based on the DT network [21]. All show link lengths relative to the reference link length.

D. Definition of Network Throughput

In this work the performance metric of interest is the network data throughput. We define data throughput as the total data transported by the network that satisfies some predefined traffic profile [11]. That is if we have a traffic profile, a matrix of elements detailing the fraction of total traffic requested between each source destination node pair, and the matrix of data rate available between each source destination node pair then the throughput is the maximum traffic as a multiplier of the traffic profile that can be transported by the network.

If $\mathbf{T}$ is a matrix defining the traffic profile with elements $T_{s,d}$ representing the fraction of traffic between source node, s, and destination node, d, where $\mathbf{T}$ is normalized such that

$$\sum_s \sum_d T_{s,d} = 1 \tag{4}$$

and $\mathbf{C}$ is a matrix defining the data transport capability with elements $C_{s,d}$ representing the available data rate between source node, s and destination node, d. $C_{s,d}$ is the sum of all the transceiver data rates, θ, providing a connection between the source and destination node pair, s, d.

Published at http://dx.doi.org/10.1109/JLT.2017.2674308

Hence the throughput is the maximum Θ such that

$$C_{s,d} \geq \Theta T_{s,d} \qquad \forall \quad s,d \tag{5}$$

This definition of throughput is similar to that used by S. A. Jyothi et al. [33] except for a slight difference in the normalization of the traffic profile, $\mathbf{T}$. The inclusion of the traffic profile constraint in the definition ensures that during network optimization easier connections are not favoured and the capability of all connections is adjusted fairly.

Throughout this paper we consider the case of a uniform all to all traffic profile with elements $T_{s,d}$ are given by

$$T_{s,d} = \begin{cases} \frac{1}{N(N-1)} & s \neq d \\ 0 & s = d \end{cases} \tag{6}$$

where N is the number of nodes. In this case the network throughput simplifies to

$$\Theta = N\,(N-1) \min_{s,d,s\neq d} C_{s,d}. \tag{7}$$

E. Calculation of Network Throughput

A number of techniques have been used to estimate and calculate the maximum throughput of computer data networks [34], [35]. For optical communications networks techniques include minimum cut to estimate throughput upper bounds, Monte-Carlo simulations to route sequential [26], [27] or dynamic demands to find the blocking load and integer linear program (ILP) based multicommodity flow solutions [36].

Cut techniques are based on the idea that where a cut divides the network into two connected subgraphs then all the traffic between the subgraphs must cross the cut. Traditional minimum cut techniques are used to find the minimum number of wavelengths required to fully connect the graph [37]. In this work we use the minimum cut technique to find the throughput upper bound given a traffic profile and the impairment limited throughput of transmissions between each node pair.

The maximum multicommodity flow is the maximum throughput where individual traffic flows between source and destination can be simultaneously transmitted through the network while satisfying the wavelength, routing and impairment constraints.

The maximum network throughput was found by optimally solving the RWA using an integer linear program (ILP). The k-shortest light paths between each node pair where pre-calculated, along with their SNR and supported data rate. The ILP allocates transmitters to light paths and wavelengths, to maximize the overall network throughput subject to the constraints imposed by the uniform traffic profile, wavelength continuity and avoidance of wavelength collisions being satisfied [36]. The time required to compute the solution can be reduced by providing the linear program solver with tight upper bounds and for this the minimum cut technique proved useful.

Consider the network topology defined by the graph $G(V,E)$ with a set V of vertices formed of ROADMs and a set E of edges formed of fiber pairs. The cut technique requires that the graph be divided into two sub-graphs $G_1(V_1,E_1)$ and $G_2(V_2,E_2)$ by cutting E_C edges. That is E is the full set of edges, $E := E_1 \cup E_2 \cup E_C$ and V is the full set of vertices $V := V_1 \cup V_2$. The two sub-graphs, $i \in \{1,2\}$ are connected such that signals from source node $s \in V_i$ to destination node $d \in V_i$ can be routed over the links $e \in E_i$. The total network throughput is calculated in proportion with the traffic profile from the maximum traffic between the two sub-graphs routed across the cut links $e \in E_C$. The minimum cut is the cut which minimizes the total network throughput. This estimate of the network throughput from the minimum cut is an upper bound of the maximum multicommodity flow based on an optimal ILP solution of the routing and wavelength assignment [35]. Finding the minimum cut is also an NP hard problem however enumerating over all possible cuts can to be completed in a short time for moderate sized networks.

The maximum network throughput constrained by the links, $e \in E_C$, between the two sub-graphs is calculated as follows. Firstly the shortest path route between all the source nodes $s \in V_1$ and all the destination nodes $d \in V_2$ is calculated using Dijkstra's algorithm. Given the shortest path we calculate the quality of transmission over this path using the impairment model to get the received symbol SNR. Then using the transceiver model the data rate capability $\theta_{s,d}$ of a transceiver utilizing the shortest path can be calculated.

Firstly if we allow fractional channel bandwidth assignments[1], then for a throughput upper bound, Θ_f, the required bandwidth, in number of channels, for the flow between source, s, and destination, d, is given by $\Theta_f \frac{T_{s,d}}{\theta_{s,d}}$. Equating the total required bandwidth for the flows across the network cut to the available bandwidth in the cut links then this minimum cut network throughput is given by Θ_f as

$$\Theta_f = \min_{E_C} \left\lfloor |E_C|\ W \left(\sum_{s\in V_1, d\in V_2} \frac{T_{s,d}}{\theta_{s,d}} \right)^{-1} \right\rfloor \tag{8}$$

where E_C is the set of links in the minimum cut, $|E_C|$ is the number of links cut and W is the number of channels, 80, in each link.

Applying the integer constraint on the allocation of transceivers and channels, then for a network throughput Θ', the bandwidth required for the flow between the two subnets is given by $\sum_{s\in V_1, d\in V_2} \left\lceil \Theta' \frac{T_{s,d}}{\theta_{s,d}} \right\rceil$, where $\lceil x \rceil$ is defined as the smallest integer greater or equal to x. This required bandwidth must be less than the available bandwidth across the cut given by $|E_C|\ W$. We introduce an indicator function, $I\left(\Theta', E_C\right)$ given by

$$I\left(\Theta', E_C\right) = \begin{cases} 1, & \text{if} \quad \sum_{s\in V_1, d\in V_2} \left\lceil \Theta' \frac{T_{s,d}}{\theta_{s,d}} \right\rceil \leq |E_C|\ W \\ 0, & \text{otherwise.} \end{cases} \tag{9}$$

The minimum cut maximum network throughput, the upper bound of the multicommodity flow based maximum throughput, Θ_{UB} is found by solving

$$\Theta_{UB} = \min_{E_C} \left[\max_{\Theta'} \left(\Theta' \cdot\ I\left(\Theta', E_C\right) \right) \right]. \tag{10}$$

[1]That is we allow a transceiver to operate between source and destination utilizing only a fraction of a channel bandwidth. This is not allowed in our fixed grid approach but removes the integer constraint giving an upper bound.

The inner part of (10) was solved iteratively over Θ', while the outer part of (8) and (10) was solved by enumerating over all connected sub-graphs $G_1(V_1, E_1)$, $G_2(V_2, E_2)$. Finally the network throughput, Θ, was found using an ILP to solve the multicommodity flow RWA and imposing the constraint $\Theta \leq \Theta_{UB}$.

To summaries Θ_f is the maximum throughput estimated from a minimum cut where there has been a fractional assignment of channel bandwidth, while Θ_{UB} is the maximum throughput estimated from a minimum cut where there has been an integer assignment of channel bandwidth. Both minimum cut results are upper bounds since the exact routing assignment is not made and wavelength continuity is not constrained. Only that the total capacity between subnets will satisfy the total demand between subnets. Θ is the maximum multicommodity flow calculated using a fully constrained ILP and represents the maximum network throughput. $\Theta \leq \Theta_{UB} \leq \Theta_f$. We could also insert an estimation based on a wavelength continuity relaxed ILP between Θ and Θ_{UB}. The order of these results can be intuitively understood as in moving from the right most Θ_f with minimal constraints each move left adds additional constraints until Θ contains all routing, wavelength and integer channel allocation constrains.

III. Results

The physical layer impairment model, transceiver model and throughput estimation techniques described in section II were used to calculate the network benefits of reducing the coding gap, reducing the data rate adaptation quantization and considering the advantages of digital nonlinear impairment mitigation.

A. Reduction of Coding Gap

We consider the case where an improvement in the transceiver coding and modulation allows the data rate to more closely approach the Shannon limit. Beginning with a transceiver that exhibits a 3 dB SNR gap to the Shannon capacity that is improved to be an ideal Shannon capacity transceiver we calculate the data throughput of the three test topologies for the two coding gaps. In the case of the 3-node network and the DT network we calculate the upper bound for a fractional channel bandwidth assignment using the minimum cut technique, using equation (8) and also the actual maximum throughput based on an analytical solution for the 3-node linear network and an ILP multicommodity flow approach for the 9-node DT network.

Figure 2 shows the maximum throughput for the three topologies as a function of the length scale. The fractional channel bandwidth assigned result shows a smooth upper bound that decreases as the network length scale is increased. The integer channel ILP multicommodity flow is equal to or less than the minimum cut fractional channel bandwidth assigned throughput, Θ_f, as there may be some unused channels, when there is insufficient spare channels to increase all the data flows fairly.

Figure 3 compares the relative increase in network throughput for the three topologies. Good agreement was found between the gain in fractional channel bandwidth assigned minimum cut upper bound when the length scale was calculated as the mean shortest path across the minimum cut.

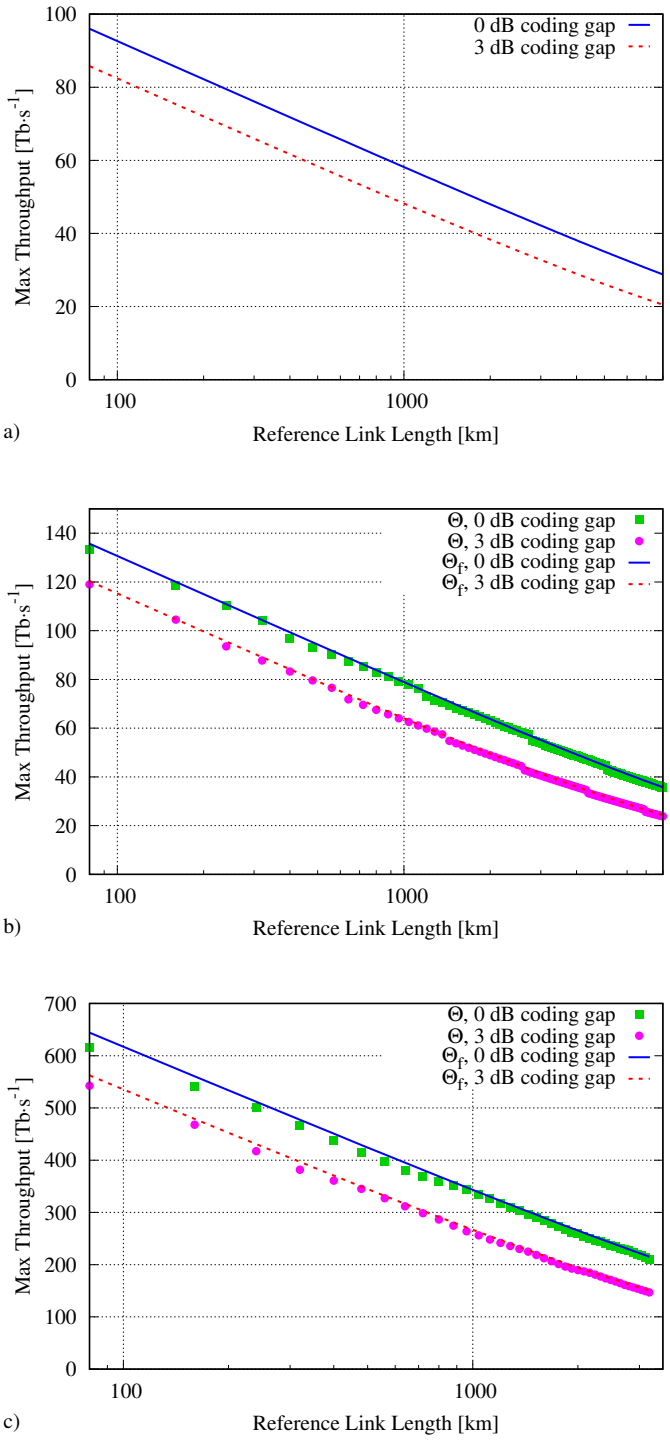

Fig. 2. Comparison of maximum throughput for ideal and non-ideal Shannon capacity transceivers as a function of length. The transceivers have a continuous rate adaptation. For a) a point-to-point link, b) a 3-node network and c) the DT network. The continuous lines show fractional channel bandwidth assigned, minimum cut upper bounds, Θ_f, while symbols show integer channel maximum multicommodity flow results, Θ. Note for a point-to-point link $\Theta = \Theta_f$ as there is only one flow and one route and as such all channels are assigned fully to that flow.

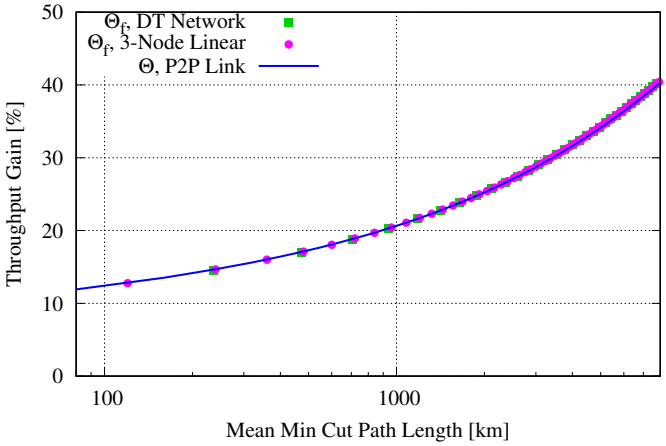

Fig. 3. The gain in maximum throughput obtained by reducing the transceiver coding gap from 3 to 0 dB as a function of the length scale. It shows that for ideal fractional channel bandwidth assignment, continuous transceiver rate adaptation and a length scale based on the mean path length across the minimum network cut, the network throughput gain is equal to that of a point-to-point link.

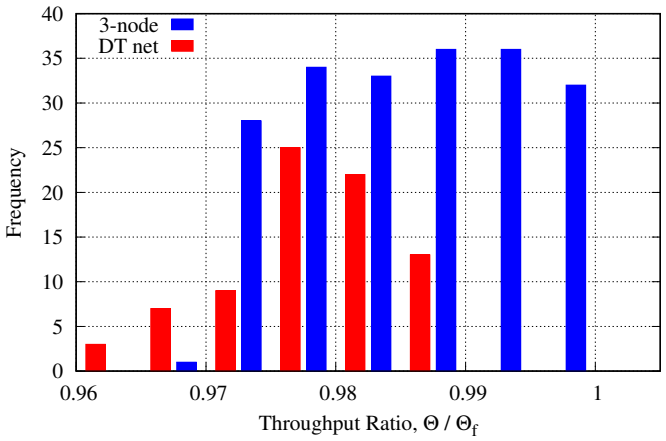

Fig. 4. Histogram showing the distribution of the ratio of maximum throughput for integer channel RWA compared to ideal fractional channel bandwidth assignments. For the 3-node and DT networks with continuous transceiver rate adaptation.

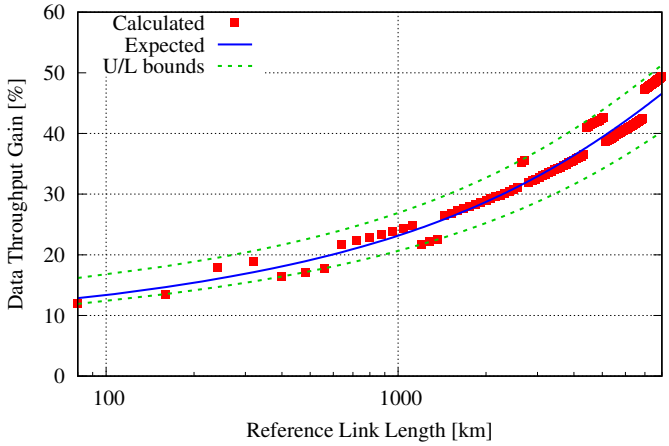

Fig. 5. 3-node linear network throughput gain when the transceiver coding gap is reduced from 3 to 0 dB in the case of integer channel RWA, multicommodity flow result for continuous transceiver rate adaptation. Also shown are the expected gain and upper and lower bounds due to the integer channel constraint.

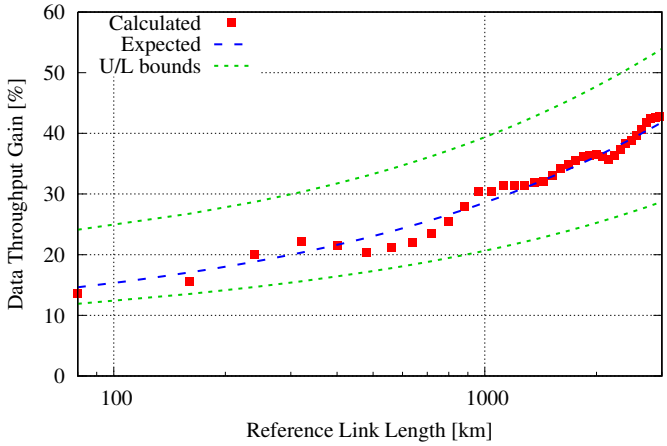

Fig. 6. DT network throughput gain when the transceiver coding gap is reduced from 3 to 0 dB in the case of integer channel RWA, multicommodity flow result for continuous transceiver rate adaptation. Also shown are the expected gain and upper and lower bounds due to the integer channel constraint.

For the topologies studied, this suggests that in an idealized fractional bandwidth routed network the increase in network throughput achieved by improving the transceiver coding can be estimated from a point-to-point link with length equal to the average path length across the minimum cut. If we then move to an integer channel multicommodity flow solution we know the network throughput will be reduced as previously shown in figure 2, b) and c). Figure 4 shows the histogram of the ratio of the integer channel multicommodity flow to the fractional channel minimum cut upper bound for the 3-node and DT networks. For the 3-node network there are two bidirectional flows across the minimum cut and thus two flows compete for bandwidth in each fiber giving the routing one degree of freedom. The histogram of the ratio between the fractional channel and integer channel solutions shows a near uniform distribution with a mean 0.9855 and standard deviation 0.0085. This is comparable to either flow being within half a channel of the optimum $\approx \frac{39.5}{40} = 0.9875$ with a variation given by a uniform distribution with standard deviation $\approx \frac{0.5}{40\sqrt{3}} = 0.0072$. For the DT network there are 18 bidirectional flows across the minimum cut that cuts four fibers, 320 channels. The distribution of the DT network results in figure 4 depends on the competition for bandwidth between the 18 bidirectional flows with 5 different lengths and has a mean 0.9782 and standard deviation 0.0068. This is comparable to each flow being within half a channel of the optimum giving an expected mean of $\approx \frac{17.5}{18} = 0.9722$ and a standard deviation due to the four degrees of freedom of $\approx \frac{0.5}{18\sqrt{3}}\frac{1}{\sqrt{4}} = 0.0080$.

It is interesting to consider the bounds on the network throughput gains when the RWA is constrained to integer channels. We have already seen that the mean throughput gain follows the gain of a point-to-point link with length equal to the mean path length across the minimum network cut. The

TABLE III
MEAN LOST CAPACITY PER TRANSCEIVER

	Loss per transceiver [Gb·s^{-1}]			
Quantisation	100 Gb·s^{-1}		25 Gb·s^{-1}	
P2P Link	51.2	± 32.5	12.2	± 7.1
3 Node Network	55.8	± 16.7	12.1	± 5.9
DT Network	59.4	± 11.5	14.0	± 4.8

lower bound for data throughput gain is limited by the gain in the worst light path when the RWA solution remains unaltered. That is the overall network throughput increases in proportion with the gains in the worst improved light path. The upper bound on the throughput gain occurs when in the initial case the RWA is 1 channel below optimum for the shortest path across the minimum network cut. Thus when the transceiver rate is improved the network throughput increases proportion with the average gains and the gain due to 1 extra channel in this shortest flow. Figures 5 and 6 show the gains in network throughput as the transceiver is improved from a 3 dB coding gap to an ideal Shannon capacity along with the lower bound, expected and upper bounds for the anticipated throughput gains. It can be seen for the 3-node network these bounds tightly fit the data while for the DT network the larger number and variation of path length leads to a lower probability that the throughput gains will deviate from the mean and approach the bounds.

B. Quantization of Transceiver Throughput

An important consideration with adaptive transceivers is how finely must the parameters be adapted? To understand the effect of the granularity of the adaptation on the network throughput the three topologies were tested with ideal Shannon rate transceivers, coding gap 0 dB with $g = 1$, where the rate was either adapted continuously or quantized to give data rates in steps of either 100 or 25 Gb·s^{-1}. Figure 7 shows the maximum throughput for the three topologies as a function of length scale for the three transceiver adaptation granularities.

To compare the three networks we consider the maximum throughput gap between the quantized and continuous adaptation per transceiver. For the point-to-point link there are 160 active transceivers, for the 3 node network an average of 228 active transceivers and for the DT network an average of 1210 active transceivers. Table III shows the throughput loss per transceiver for 100 and 25 Gb·s^{-1} quantization for the three topologies. It can be seen the average loss per transceiver is approximately half the quantization steps while the standard deviation of the loss is considerably reduced in the network case where the large variation of path lengths renders the extreme values less likely.

The advantages of finer transceiver adaptation is known and recently assessed by a number of authors [18], [19]. It is an important consideration in the design of adaptive transceivers and we highlight here the general result relating to the average loss of throughput per transceiver. This allows some quantifiable estimation for the trade-offs in adaptive transceiver design.

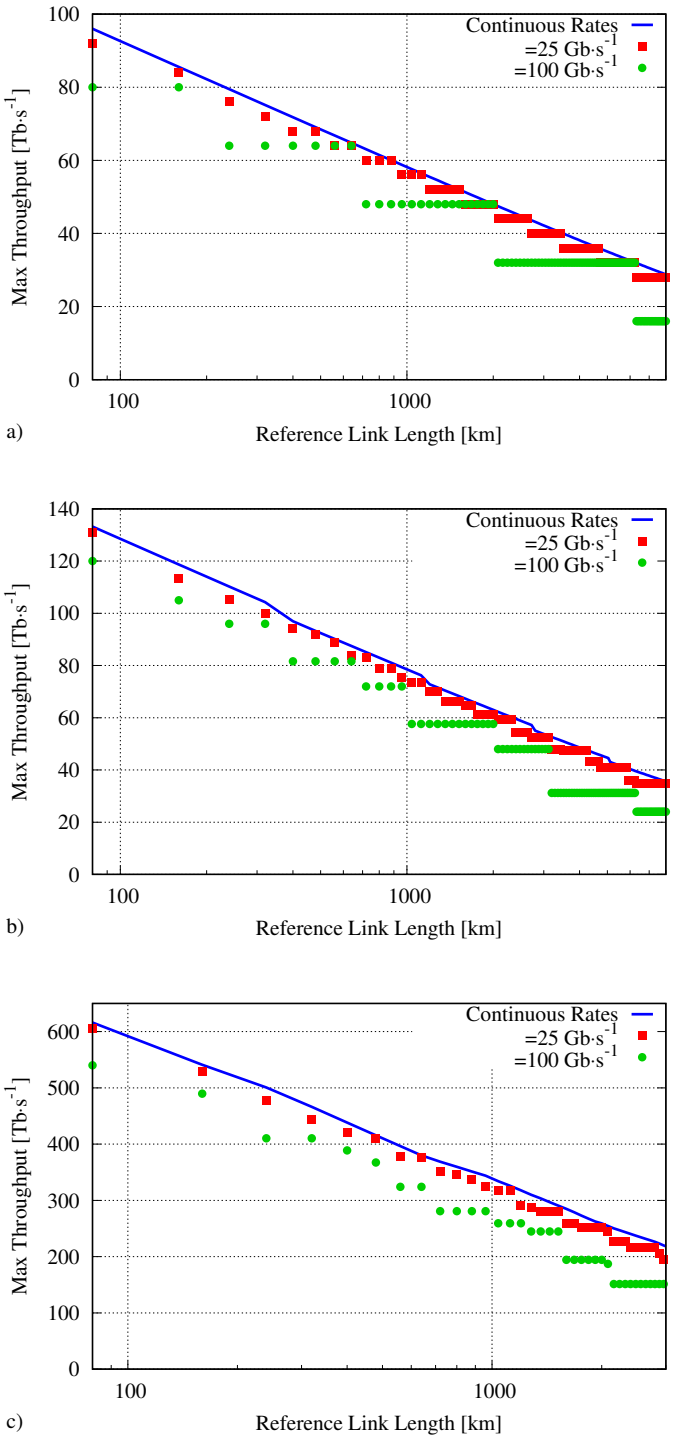

Fig. 7. Maximum throughput, Θ, the maximum multicommodity flow calculated using ILP, as a function of length. Comparing the three transceiver adaptation quantization steps for a) a point-to-point link, b) a 3-node network and c) the DT network.

C. Nonlinear Digital Mitigation

We consider the case where the transmitted signal SNR is improved by ideal digital nonlinear mitigation, for example digital back propagation, DBP. In the network case the transceiver only has full knowledge of signals transmitted together from source to destination nodes. As shown in table II,

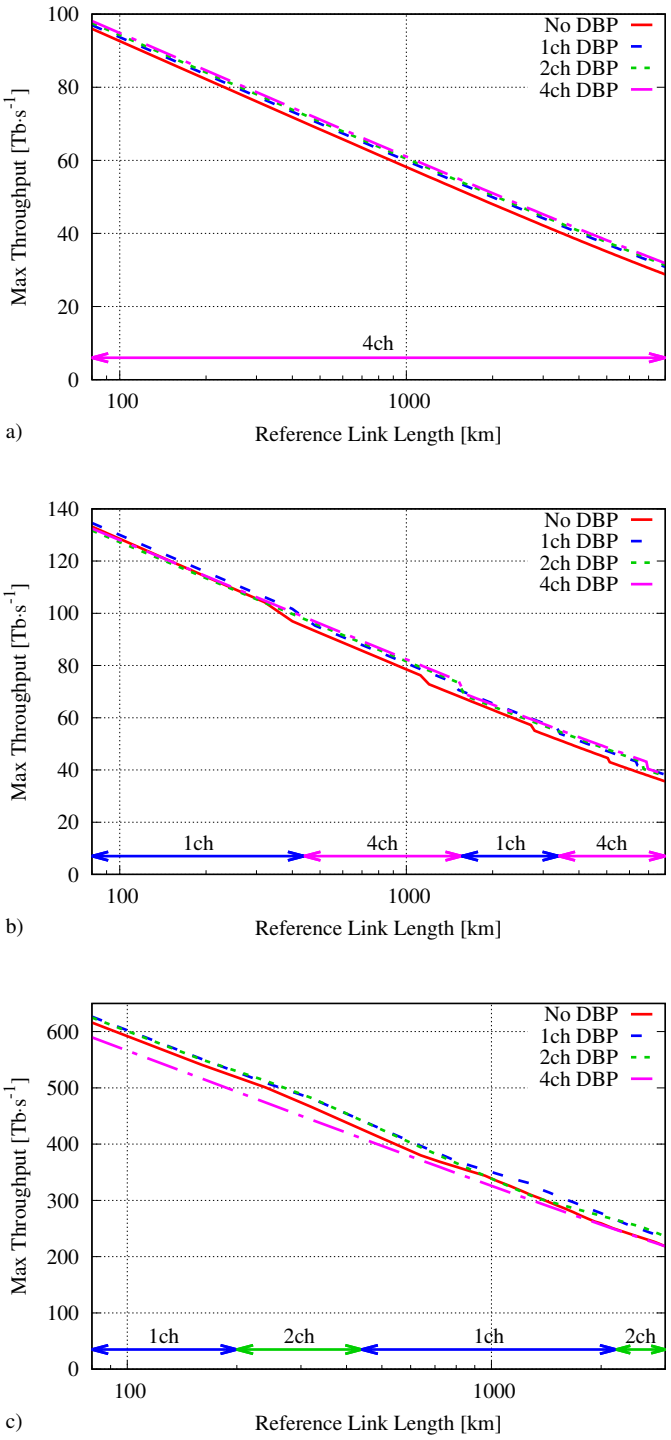

Fig. 8. Maximum throughput as a function of length for ideal DBP. These are maximum multicommodity flow results for transceivers with continuous rate adaptation. Comparing the effects of DBP and multichannel DBP for 0,1,2 and 4 grouped channels for a) a point-to-point link, b) a 3-node network and c) the DT network. Also indicated is the regions where each number of back propagated channels performs best.

and similar to [38], single channel DBP will only improve the SNR by approximately 0.6 dB. To improve the nonlinear mitigation further requires multichannel DBP, but in that case the channels must be routed together as a superchannel. We consider superchannels formed of 2 or 4 channels, where all

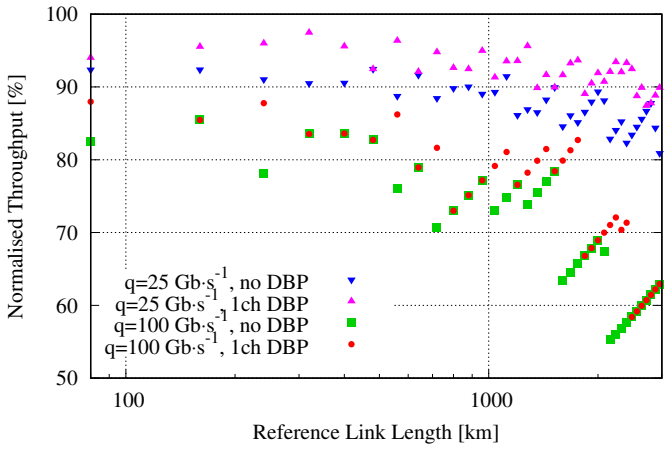

Fig. 9. Normalised maximum network throughput for the DT network as a function of the shortest link length. Results have been normalised to the upper bound estimated from the minimum cut with fractional channel bandwidth allocation, continuous rate adaptation and single channel DBP. The results shown are maximum mutlicommodity flow network throughput with and without single channel DBP for rate adaption quantized in 25 Gb·s^{-1} and 100 Gb·s^{-1}.

the signals are routed as superchannels so that all benefit from the DBP. The worst case SNR of a central superchannel in a fully loaded link improves by 0.8 dB and 1.0 dB for the 2 and 4 channel superchannels respectively. These SNR gains are comparable to those suggested in [38]. This improves the throughput of the point-to-point link as shown in figure 8 a) with larger multichannel DBP superchannels giving ever increased throughput. For the case of a wavelength routed network the grouping of channels into superchannels reduces the number of routed entities and leads to a loss of throughput where the RWA cannot divide the bandwidth optimally. Figures 8 b) and c) show the throughput for the 3-node linear network and DT network respectively. It can be seen that the loss due to the RWA is often greater than the gains due to multichannel DBP such that single channel DBP often out performs multichannel DBP in a network context.

Figure 9 show the normalised maximum throughput achieved with and without single channel DBP when the transceiver data rate is quantized in steps of 100 and 25 Gb·s^{-1} respectively. The throughput has been normalised to Θ_f the throughput upper bound for continuous rate adaptation, with single channel DBP and fractional channel bandwidth assignment estimated from the minimum cut. It is observed that with 100 Gb·s^{-1} quantization of the transceiver data rate that in approximately half of the instances single channel DBP has no effect on throughput while in some case single channel DBP gives a substantial enhancement. However with 25 Gb·s^{-1} quantization of the transceiver data rate, single channel DBP improves the throughput in most cases. It is observed from figure 9 that moving to 25 Gb·s^{-1} quantization of the transceiver data rate is more effective than single channel DBP with 100 Gb·s^{-1} quantization.

IV. Conclusions

This paper has explored the complexities involved in assessing network throughput and the difference from simple

Published at http://dx.doi.org/10.1109/JLT.2017.2674308

point-to-point links. We have assessed throughput as a function of the length scale as a way to more fully assess network throughput and obtain a handle on the variations of throughput with network perturbations. We have described an adaptation of the minimum network cut technique to estimate an upper bound on the maximum network throughput while taking a traffic profile, transmission impairments and rate adaptation into consideration. This proved a useful tool to upper bound the ILP based multicommodity flow optimization used to calculate the maximum network throughput.

For the two simple network topologies considered we have shown that the expected gain in network throughput due to some transceiver adaptation or improvement is the same as the gain in throughput for a point-to-point link with length equal to the mean path across the minimum network cut. Introducing the integer constraint of channel allocation and quantization of the transceiver adaptation leads to a deviation of the gain in throughput from the expectation. The upper and lower bounds for the gain in throughput were also estimated. The expectation and upper and lower bounds allow an understanding of the variation of a single network result and allows such results to be placed into context. The variation suggests that to robustly estimate the gains of a particular transceiver adaptation for a particular network topology requires a study that also includes any expected perturbations and uncertainty of the physical properties.

The use of single channel digital nonlinear mitigation leads to a small improvement in SNR and thus network throughput. Better gains in SNR are achieved with multichannel digital nonlinear mitigation. However the multiple channels must be co-propagated as a superchannel taking the same route. This reduced number of larger superchannels leads to a loss of throughput where the RWA can no longer optimally divide the bandwidth resource. We have shown for the network topologies studied that this loss of throughput due to RWA is often more significant than the gains due to the better nonlinear mitigation.

It is observed for the topologies studied that the use of smaller quantization steps in the transceiver adaptation appears to improve the throughput more significantly than using digital nonlinear mitigation or making a small reduction to the coding gap. However if sufficient computation resources are available all three techniques can be combined to increase the network throughput.

Data Access

All data accompanying this publication are directly available within the publication.

References

[1] P. Poggiolini, "The GN Model of Non-Linear Propagation in Uncompensated Coherent Optical Systems," *J. Lightw. Technol.*, vol. 30, no. 24, pp. 3857–3879, Dec. 2012.

[2] K. Roberts and C. Laperle, "Flexible Transceivers," in *Proc. Eur. Conf. Optical Communications*, Amsterdam (NL), 2012, p. We.3.A.3.

[3] D. S. Millar, T. Koike-Akino, S. Ö. Ark, K. Kojima, K. Parsons, T. Yoshida, and T. Sugihara, "High-Dimensional Modulation for Coherent Optical Communications Systems," *Opt. Exp.*, vol. 22, no. 7, pp. 8798–8812, Apr. 2014.

[4] X. Zhou, L. E. Nelson, and P. D. Magill, "Rate-Adaptable Optics for next Generation Long-Haul Transport Networks," *IEEE Commun. Mag.*, vol. 51, no. 3, pp. 41–49, 2013.

[5] M. S. Moreolo, J. M. Fabrega, L. Nadal, F. J. V, A. Mayoral, R. Vilalta, R. Mu, R. Casellas, R. Mart, M. Nishihara, T. Tanaka, T. Takahara, J. C. Rasmussen, C. Kottke, M. Schlosser, R. Freund, F. Meng, S. Yan, and G. Zervas, "SDN-Enabled Sliceable BVT Based on Multicarrier Technology for Multiflow Rate / Distance and Grid Adaptation," *J. Lightw. Technol.*, vol. 34, no. 6, pp. 1516–1522, Mar. 2016.

[6] F. Buchali, F. Steiner, G. Bocherer, L. Schmalen, P. Schulte, and W. Idler, "Rate Adaptation and Reach Increase by Probabilistically Shaped 64-QAM: An Experimental Demonstration," *J. Lightw. Technol.*, vol. 34, no. 7, pp. 1599–1609, Apr. 2015.

[7] T. Fehenberger, D. Lavery, R. Maher, A. Alvarado, P. Bayvel, and N. Hanik, "Sensitivity Gains by Mismatched Probabilistic Shaping for Optical Communication Systems," *IEEE Photon. Technol. Lett.*, vol. 28, no. 7, pp. 786–789, Apr. 2016.

[8] G.-H. Gho and J. M. Kahn, "Rate-Adaptive Modulation and Coding for Optical Fiber Transmission Systems," *J. Lightw. Technol.*, vol. 30, no. 12, pp. 1818–1828, June 2012.

[9] D. A. A. Mello, A. N. Barreto, T. C. de Lima, T. F. Portela, L. Beygi, and J. M. Kahn, "Optical Networking With Variable-Code-Rate Transceivers," *J. Lightw. Technol.*, vol. 32, no. 2, pp. 257–266, Jan. 2014.

[10] L. Beygi, E. Agrell, J. M. Kahn, and M. Karlsson, "Rate-Adaptive Coded Modulation for Fiber-Optic Communications," *J. Lightw. Technol.*, vol. 32, no. 2, pp. 333–343, Jan. 2014.

[11] A. Alvarado, D. J. Ives, S. J. Savory, and P. Bayvel, "On the Impact of Optimal Modulation and FEC Overhead on Future Optical Networks," *J. Lightw. Technol.*, vol. 34, no. 9, pp. 2339–2352, May 2016.

[12] D. J. Ives, P. Bayvel, and S. J. Savory, "Assessment of Options for Utilizing SNR Margin to Increase Network Data Throughput," in *Proc. Optical Fiber Communications Conf.*, Los Angeles, CA. (USA), Mar. 2015, p. M2I.3.

[13] ——, "Routing, Modulation, Spectrum and Launch Power Assignment to Maximize the Traffic Throughput of a Nonlinear Optical Mesh Network," *Photon. Netw. Commun.*, vol. 29, no. 3, pp. 244–256, Mar. 2015.

[14] E. Ip and J. M. Kahn, "Compensation of Dispersion and Nonlinear Impairments Using Digital Backpropagation," *J. Lightw. Technol.*, vol. 26, no. 20, pp. 3416–3425, Oct. 2008.

[15] R. Maher, T. Xu, L. Galdino, M. Sato, A. Alvarado, K. Shi, S. J. Savory, B. C. Thomsen, R. I. Killey, and P. Bayvel, "Spectrally Shaped DP-16QAM Super-Channel Transmission with Multi-Channel Digital Back-Propagation," *Scientific Reports*, vol. 5, no. 8214, pp. 1–8, Feb. 2015.

[16] O. Gerstel, M. Jinno, A. Lord, and S. J. B. Yoo, "Elastic Optical Networking: A New Dawn for the Optical Layer?" *IEEE Commun. Mag.*, vol. 50, no. 2, pp. s12–s20, Feb. 2012.

[17] N. Sambo, P. Castoldi, A. D'Errico, E. Riccardi, A. Pagano, M. S. Moreolo, J. M. Fabrega, D. Rafique, A. Napoli, S. Frigerio, E. H. Salas, G. Zervas, M. Nolle, J. K. Fischer, A. Lord, and J. P. F.-P. Gimenez, "Next Generation Sliceable Bandwidth Variable Transponders," *IEEE Commun. Mag.*, vol. 53, no. 2, pp. 163–171, Feb. 2015.

[18] M. Ghobadi, J. Gaudette, R. Mahajan, A. Phanishayee, B. Klinkers, and D. Kilper, "Evaluation of Elastic Modulation Gains in Microsoft's Optical Backbone in North America," in *Proc. Optical Fiber Communication Conf.*, Anaheim, CA. (USA), Mar. 2016, p. M2J.2.

[19] D. J. Ives, P. Wright, A. Lord, and S. J. Savory, "Using 25 GbE Client Rates to Access the Gains of Adaptive Bit- and Code-Rate Networking," *J. Opt. Commun. Netw.*, vol. 8, no. 7, pp. A86–A91, July 2016.

[20] S. K. Korotky, R.-J. Essiambre, and R. W. Tkach, "Expectations of Optical Network Traffic Gain Afforded by Bit Rate Adaptive Transmission," *Bell Labs Technical Journal*, vol. 14, no. 4, pp. 285–295, Feb. 2010.

[21] S. Makovejs, C. Behrens, R.-P. Braun, S. Ten, C. Towery, I. Roudas, K. Koreshkov, T. Nath, and A. Gladisch, "Impact of Adaptive-Rate Transponders and Fiber Attributes on the Achievable Capacity," *J. Opt. Commun. Netw.*, vol. 7, no. 3, pp. 172–175, Feb. 2015.

[22] H. Beyranvand and J. A. Salehi, "A Quality-of-Transmission Aware Dynamic Routing and Spectrum Assignment Scheme for Future Elastic Optical Networks," *J. Lightw. Technol.*, vol. 31, no. 18, pp. 3043–3054, Sep. 2013.

[23] H. Cukurtepe, M. Tornatore, A. Yayimli, and B. Mukherjee, "Provisioning of Dynamic Traffic in Mixed-Line-Rate Optical Networks with Launch Power Determination," *Photon. Netw. Commun.*, vol. 27, no. 3, pp. 154–166, Apr. 2014.

[24] T. Takagi, H. Hasegawa, K.-i. Sato, Y. Sone, B. Kozicki, A. Hirano, and M. Jinno, "Dynamic Routing and Frequency Slot Assignment for Elastic

Optical Path Networks that Adopt Distance Adaptive Modulation," in *Proc. Optical Fiber Communication Conf.*, (USA), 2011, p. OTuI.7.

[25] N. Sambo, G. Meloni, F. Cugini, F. Fresi, A. D'Errico, L. Poti, P. Iovanna, and P. Castoldi, "Routing, Code, and Spectrum Assignment, Subcarrier Spacing, and Filter Configuration in Elastic Optical Networks [Invited]," *J. Opt. Commun. Netw.*, vol. 7, no. 11, p. B93, Oct. 2015.

[26] P. Wright, A. Lord, and S. Nicholas, "Comparison of Optical Spectrum Utilization Between Flexgrid and Fixed Grid on a Real Network Topology," in *Proc. Optical Fiber Communication Conf.*, Los Angeles, CA. (USA), 2012, p. OTh3B.5.

[27] M. Cantono, R. Gaudino, and V. Curri, "Potentialities and Criticalities of Flexible-Rate Transponders in DWDM Networks: A Statistical Approach," *J. Opt. Commun. Netw.*, vol. 8, no. 7, p. A76, July 2016.

[28] D. J. Ives, A. Alvarado, and S. J. Savory, "Adaptive Transceivers in Nonlinear Flexible Networks," in *Proc. Eur. Conf. Optical Communications*, Düsseldorf (DE), 2016, p. M.1.B.1.

[29] A. Morea, J. Renaudier, T. Zami, A. Ghazisaeidi, and O. Bertran-Pardo, "Throughput Comparison Between 50-GHz and 375-GHz Grid Transparent Networks [Invited]," *J. Opt. Commun. Netw.*, vol. 7, no. 2, p. A293, Feb. 2015.

[30] J. M. Fabrega, M. Svaluto Moreolo, L. Martín, A. Chiadò Piat, E. Riccardi, D. Roccato, N. Sambo, F. Cugini, L. Potì, S. Yan, E. Hugues-Salas, D. Simeonidou, M. Gunkel, R. Palmer, S. Fedderwitz, D. Rafique, T. Rahman, H. de Waardt, and A. Napoli, "On the Filter Narrowing Issues in Elastic Optical Networks," *J. Opt. Commun. Netw.*, vol. 8, no. 7, p. A23, Jul. 2016.

[31] P. Poggiolini, G. Bosco, A. Carena, R. Cigliutti, V. Curri, F. Forghieri, R. Pastorelli, and S. Piciaccia, "The LOGON Strategy for Low-Complexity Control Plane Implementation in New-Generation Flexible Networks," in *Proc. Optical Fiber Communication Conf.*, Anaheim, CA. (USA), 2013, p. OW1H.3.

[32] D. J. Ives and S. J. Savory, "How Pessimistic is a Worst-Case SNR Degradation as a Link Abstraction Metric ?" in *Proc. Optical Fiber Communication Conf.*, Anaheim, CA. (USA), Mar. 2016, p. Tu3F.6.

[33] S. A. Jyothi, A. Singla, P. B. Godfrey, and A. Kolla, "Measuring Throughput of Data Center Network Topologies," *ACM SIGMETRICS Performance Evaluation Review*, vol. 42, no. 1, pp. 597–598, June 2014.

[34] ——, "Measuring and Understanding Throughput of Network Topologies," *arXiv*, p. 1402.2531, Feb. 2014.

[35] M. Adler, N. J. A. Harvey, K. Jain, R. Kleinberg, and A. Rasala, "On the Capacity of Information Networks," in *SODA '06 Proceedings of the seventeenth annual ACM-SIAM symposium on Discrete algorithm*, Miami (FL) USA, 2006, pp. 241–250.

[36] D. J. Ives, P. Bayvel, and S. J. Savory, "Adapting Transmitter Power and Modulation Format to Improve Optical Network Performance Utilizing the Gaussian Noise Model of Nonlinear Impairments," *J. Lightw. Technol.*, vol. 32, no. 21, pp. 3485–3494, Nov. 2014.

[37] S. Baroni and P. Bayvel, "Wavelength Requirements in Arbitrarily Connected Wavelength-Routed Optical Networks," *J. Lightw. Technol.*, vol. 15, no. 2, pp. 242–251, Feb. 1997.

[38] R. Dar and P. J. Winzer, "On the Limits of Digital Back-Propagation in Fully Loaded WDM Systems," *IEEE Photon. Technol. Lett.*, vol. 28, no. 11, pp. 1253–1256, June 2016.

David J. Ives (S'13–M'16) received the B.Sc. degree in Physics from the University of Birmingham UK, in 1988 and the M.Res. degree in Photonic Systems Development (with distinction) from University College London UK, in 2011. In 2015, he completed a Ph.D. with the Optical Networks Group in the Department of Electronic and Electrical Engineering at University College London, U.K.

Dr. Ives is currently a post-doctoral researcher at the University of Cambridge. Between 1988–2010 he was at the National Physical Laboratory in Teddington, UK, as part of the Photonics group, where he developed techniques for the characterization of optical fiber waveguides and the calibration of optical fiber test equipment. He was the recipient of the 2014 Conference on Optical Network Design and Modeling best poster award. His current interests are optical communications, physical layer network optimization and physical layer abstraction and virtualisation.

Alex Alvarado (S'06–M'11–SM'15) was born in Quellón, on the island of Chiloé, Chile. He received his Electronics Engineer degree (Ingeniero Civil Electrónico) and his M.Sc. degree (Magíster en Ciencias de la Ingeniería Electrónica) from Universidad Técnica Federico Santa María, Valparaíso, Chile, in 2003 and 2005, respectively. He obtained the degree of Licentiate of Engineering (Teknologie Licentiatexamen) in 2008 and his PhD degree in 2011, both of them from Chalmers University of Technology, Gothenburg, Sweden.

Dr. Alvarado is currently a tenure-track assistant professor at the Signal Processing Systems (SPS) Group, Department of Electrical Engineering, Eindhoven University of Technology (TU/e), The Netherlands. During 2014-2016, he was a Senior Research Associate at the Optical Networks Group, University College London, United Kingdom. In 2012–2014 he was a Marie Curie Intra-European Fellow at the University of Cambridge, United Kingdom, and during 2011–2012 he was a Newton International Fellow at the same institution. Dr. Alvarado is a recipient of the 2009 IEEE Information Theory Workshop Best Poster Award, the 2013 IEEE Communication Theory Workshop Best Poster Award, and the 2015 IEEE Transaction on Communications Exemplary Reviewer Award. He is a senior member of the IEEE and an associate editor for IEEE Transactions on Communications (Optical Coded Modulation and Information Theory). His general research interests are in the areas of digital communications, coding, and information theory.

Seb J. Savory (M07–SM11–F17) received the M.Eng., M.A., and Ph.D. degrees in engineering from the University of Cambridge, U.K., in 1996, 1999, and 2001, respectively, and the M.Sc. (Maths) degree in mathematics from the Open University, Milton Keynes, U.K., in 2007.

His interest in optical communications began in 1991, when he joined STL (subsequently Nortel) in Harlow, U.K. Having been sponsored by Nortel through his undergraduate and postgraduate studies, he rejoined the Harlow Laboratories in 2000. In 2005, he moved to UCL where he held a Leverhulme Trust Early Career Fellowship from 2005 to 2007, before being appointed as a Lecturer (2007), Reader (2012) and Professor (2015). During 2014/15 he held a RAEng / Leverhulme Trust Senior Research Fellowship and was a joint recipient of the RAEng Colin Campbell Mitchell Award in 2015. In October 2015, he was elected as a Fellow of Churchill College, Cambridge and in January 2016 moved to Cambridge as a University Lecturer.

Dr. Savory is the Editor-in-Chief of IEEE Photonics Technology Letters and serves on the Steering Committee of the Optical Fiber Communication conference having previously served as a General Chair (2015) and Program Chair (2013). He is a Chartered Engineer and Fellow of the Institution of Engineering and Technology, U.K. Recently he was elevated to Fellow of the OSA and the IEEE for contributions to digital coherent transceivers for optical fiber communication.